

# Transverse and Longitudinal Beam Diagnostics using Transition Radiation \*

S. Döbert, R. Eichhorn, H. Genz, H.-D. Gräf, R. Hahn, T. Hampel, S. Kostial, H. Loos, M. Reichenbach, A. Richter, V. Schlott, E. Spamer, A. Stascheck, M. Thomas, O. Titze, T. Wesp  
 Institut für Kernphysik, TH-Darmstadt, Schlossgartenstrasse 9, D-64289 Darmstadt, Germany

## Abstract

The broad spectrum of transition radiation emitted from a thin foil in the beamline carries in principle all the properties of the beam, producing it. The optical part of the spectrum (OTR) allows to extract the transverse beam information via beamspot imaging with the use of commercial CCD cameras. The combination of a CCD and graphical data processing tools provides the operator the transverse beam parameters fast and in a comfortable way. The energy spread of the electron beam is determined with the same system by projecting the energy distribution on a transverse axis in a dispersive section of the beamline. Transition radiation in the far infrared enables bunch length measurements in the ps range with an autocorrelation technique. The bunch length was measured to be  $(4 \pm 0.25)$ ps, this was confirmed by a streak camera measurement.

## 1 INTRODUCTION

A charged particle moving through an inhomogeneity relative to the electromagnetic properties of the matter emits transition radiation, as predicted by I.M.Frank and V.L.-Ginzburg[1] in 1946. In the meantime the phenomenon is well established within electromagnetic theory[2, 3] and its application for beam diagnostics was first demonstrated in the pioneering work by L.Wartski[4]. The availability of inexpensive position sensitive detectors made transition radiation a preferable tool for beam diagnostics[5]. A charged particle crossing a single boundary emits transition radiation into the backward and forward hemisphere of the boundary. The radiation is emitted in a small cone with an opening angle of  $1/\gamma$  for relativistic particles as indicated in Fig.3 for a single foil. Equation (1) where  $\alpha$  is the fine structure constant,  $\gamma$  the Lorentz factor and  $\theta$  the emission angle with respect to the beam axis, describes the intensity distribution in the forward hemisphere for a single highly relativistic electron passing through a material with plasma frequency  $\omega_p$  into vacuum.

$$\frac{d^2W}{d\omega d\Omega} = \frac{\alpha}{\pi^2} \left( \frac{\theta}{\gamma^{-2} + \theta^2 + \left(\frac{\omega_p}{\omega}\right)^2} - \frac{\theta}{\gamma^{-2} + \theta^2} \right)^2 \quad (1)$$

The radiation in the backward hemisphere has the same characteristics with respect to the angle of spectral reflection. A measurement of that pattern is sensitiv to the di-

vergence of the beam and allows energy determination. The different properties of the electron beam can be determined in different regions of the broad emitted spectrum. The working regimes are marked in Fig.1 where the calculated spectra for different beam energies are plotted. The total emitted intensity is proportional to  $\gamma$ , to the plasma frequency of the material and of course to the beam current.

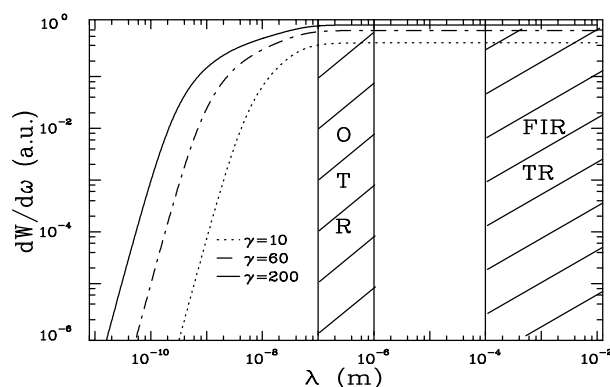


Figure 1: Spectra of transition radiation for different electron energies. The regions of OTR and FIR-TR are shaded.

## 2 OPTICAL TRANSITION RADIATION

Optical transition radiation is especially suitable for beam diagnostics because of the possibility to use CCD cameras

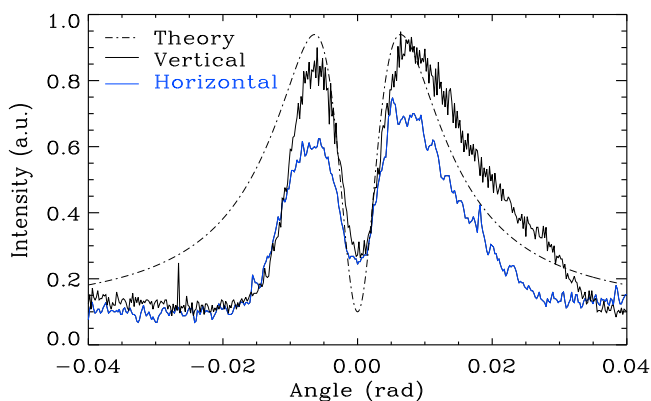


Figure 2: Horizontal and vertical profiles of the radiation pattern.

and graphical data processing. Possible observables are the

\* Supported by BMBF under contract numbers 06 DA 655 I and 05 345 EAI 3 and through a Max-Planck Research Prize.

sizes of the beam images and the shape of the radiation pattern which is visible if the optics is focused to infinity. As an example of such an imaging Fig.2 shows the horizontal and vertical profiles of the radiation pattern at  $E_0 = 80$  MeV. The position of the peaks determine the energy and the height of the central minimum is a measure of the beam divergency.

Numerous OTR diagnostics stations are installed at the S-DALINAC [6] electron accelerator to measure the transverse beam parameters routinely. The setup is sketched in Fig.3. An aluminum foil is inserted under  $45^\circ$  to allow the light detection under  $90^\circ$  with respect to the beam direction. The target material is  $25 \mu\text{m}$  thick aluminum, suc-

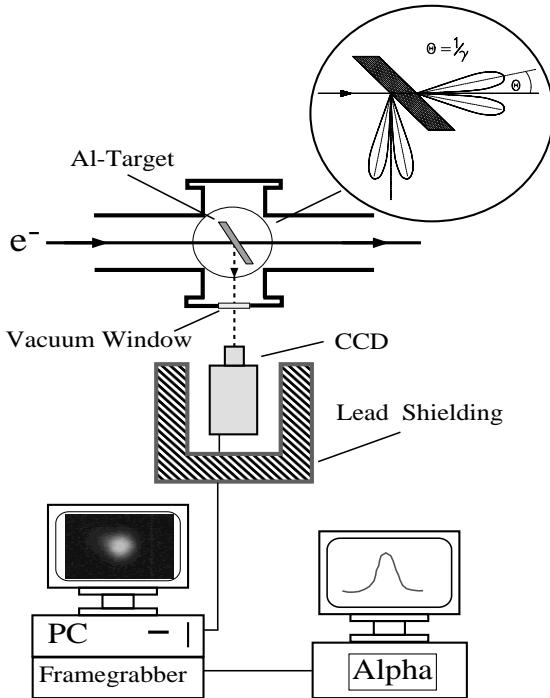


Figure 3: Schematic setup of an OTR diagnostics station.

cessful tests were also performed with silicon targets and mylar foils. Commercial CCD cameras equipped with standard  $f = 50$  mm optics are used for detection. The minimum intensity needed for these cameras is 0.05 candela. The minimum beam current needed to obtain a reasonable image shows a  $\gamma^{-1}$  dependency according to the theory. We used the system for energies ranging from 250 keV up to 120 MeV with minimum beam currents of 500 nA and 10 nA, respectively. The beam spot images are digitized by a framegrabber installed in a PC for data acquisition and controlling. The full two dimensional intensity distribution of the grabbed beamspot is finally available on an alphavox workstation for display and processing. Several routines were developed using IDL [7], a practical graphical data processing tool to extract profiles, radii, emittances and energy spread of the beam.

The OTR diagnostics system is used routinely to measure the complete set of transverse beam parameters. Figure 4

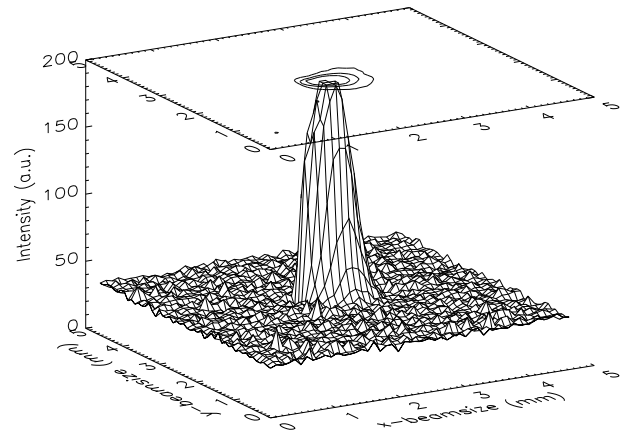


Figure 4: Intensity distribution of a grabbed beam spot image at  $E_0 = 85$  MeV. Beamsize:  $2\sigma = 0.5$  mm.

shows an example of a two dimensional distribution which is available almost online. From these distributions beam profiles can be extracted and the beamsize can be determined by a fit, assuming a Gaussian shape of the profiles. To determine the complete  $\sigma$  matrix for emittance measurements the beam radius is measured as a function of the focusing

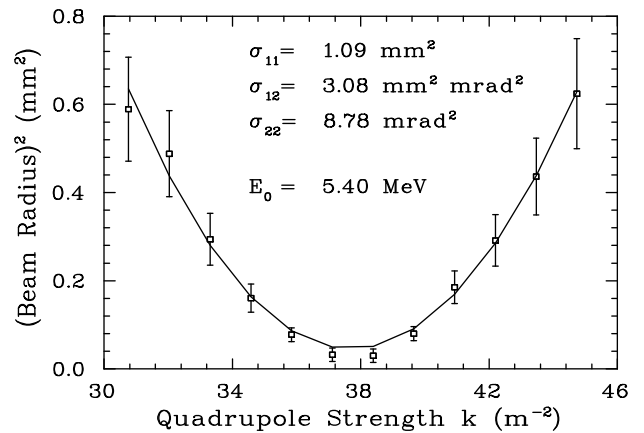


Figure 5: Example of an emittance measurement using the three-gradient method at  $E_0 = 5.4$  MeV.

strength of a quadrupole. The sigma parameters are found by fitting a quadratic form to the measured beam sizes. An example of such a measurement is presented in Fig.5. The normalized emittances were found to be  $\epsilon_{n,x} = 0.94 \pi$  mm mrad horizontally and  $\epsilon_{n,y} = 2.28 \pi$  mm mrad vertically. The measurement was performed at an energy of 5.4 MeV with a current of 500 nA and a 3 GHz cw time structure. The beam parameters could be found by fitting within an accuracy of 15 %.

The energy spread of the electron beam is proportional to its size in a dispersive section of the beamline. Taking into account the intrinsic beamsizes, measurements of the energy

distribution of the beam are also possible with the described system. With the help of a fast analysis routine it is possible to display online the energy spread. Typical measured energy distributions are of the order of  $10^{-3}$  at FWHM.

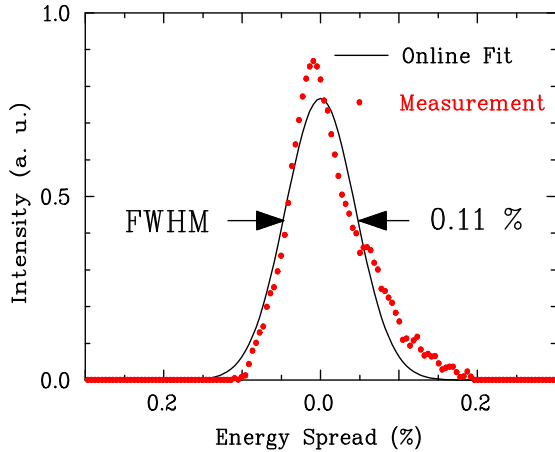


Figure 6: Energy spread determination from a beam profile measurement (background subtracted) in a dispersive section.

### 3 TRANSITION RADIATION IN THE FAR INFRARED

Bunch length measurement in the ps range is a nontrivial task with conventional techniques. The coherence of transition radiation in a region where the wavelength is comparable with the bunch length allows to profit from an autocorrelation technique[8, 9]. Since we are dealing with ps

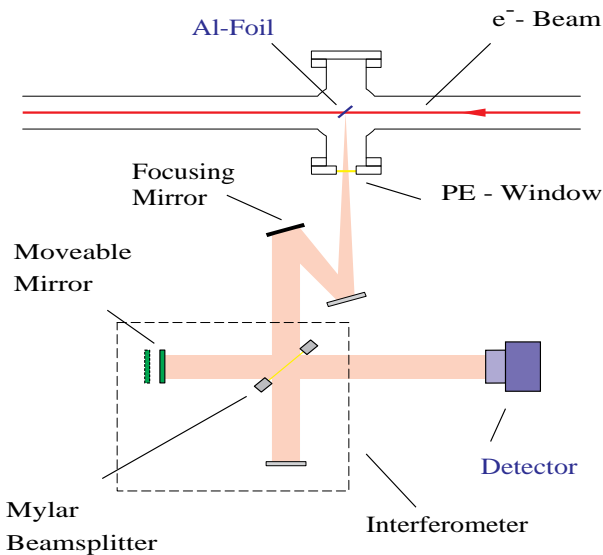


Figure 7: Autocorrelation setup for the transition radiation bunch length measurement.

bunch lengths at the S-DALINAC, our working regime is the far infrared. As sketched in Fig.7 the radiation is extracted through a PE-window, autocorrelated in a Michel-

son interferometer and finally focused on a pyroelectric detector. The power is measured as a function of the optical pathlength in one interferometer arm. A simple transformation to get the longitudinal charge distribution is not possible because the phase information is lost. A quite accurate measurement of the bunch length and the most likely bunch shape could be obtained by starting with an assumed charge distribution and a comparing analysis in frequency domain, taking into account the transfer function of the complete apparatus. Effects like water absorption and interference of beam splitter and vacuum window had to be considered carefully. The procedure is described in detail in [10]. The measurement was performed using an electron beam of 31.2 MeV energy, a bunch repetition rate of 10 MHz and a macropulse of 1 ms duration with a repetition rate of 33 Hz at an average current of  $40 \mu A$ . The measurement yielded a bunch length of  $(4 \pm 0.25)$  ps and a most likely rectangular shape.

### 4 CONCLUSION

Transition radiation has proved to be a cost efficient and comfortable alternative to viewscreens, wire scanners and SEM grids. The instantaneous and linear response over a wide range of currents and energies makes OTR preferable to viewscreens, it produces a 'true' image of the beam. Optical imaging gives the full two dimensional intensity distribution of the beam spot and results therefore in combination with fast graphical data processing in a very powerful diagnostics tool for the accelerator operator. The bunch length measurement in the ps range with a quite simple setup confirms that beam diagnostics using transition radiation has an enormous potential.

### 5 REFERENCES

- [1] V.L.Ginzburg und I.M.Frank, JETP **16** (1946) 15.
- [2] M.L.Ter-Mikaelian, *High Energy Electromagnetic Processes in Condensed Media*, Wiley-Interscience, New York (1972).
- [3] V.L.Ginzburg, Phys. Rep. **49** (1979) 1.
- [4] L.Wartski, S.Roland, J.Lasalle, M.Bolore, G.Filippi, Jour. Appl. Phys. **46** (1975) 3644.
- [5] R.Chehap, M.Taurigna, G.Bienvenu, Proc. EPAC 92, Berlin (1992) 1139.
- [6] A.Richter, Proc. EPAC 96, Barcelona (1996).
- [7] Interactive Data Language, Version 3.0, Research Systems (1993).
- [8] W.Barry, CEBAF PR-91-012 (1991).
- [9] E.R.Crosson, K.W.Berryman, T.I.Smith, R.L.Swent, H.C.Lihn, H.Wiedemann, Nucl. Instr. Meth. **A358** (1995) 216.
- [10] V.Schlott, H.Loos, H.Genz, H.-D.Gräf, R.Hahn, A.Richter, M.Thomas, T.Wesp, M.Wiencken, Part. Accel. **52** (1996) 45.